AR-006-361

HEAT FLOW CALCULATIONS FOR THE SMALL-SCALE COOKOFF BOMB TEST

D.A. JONES AND R.P. PARKER

MRL-TR-91-12

MATERIALS RESEARCH LABORATORY
DSTO

Heat Flow Calculations for the Small-Scale Cookoff Bomb Test

D.A. Jones and R.P. Parker

MRL Technical Report
MRL-TR-91-12

Abstract

This report describes the temperature distribution within the Small-scale Cookoff Bomb (SCB) test apparatus from both an experimental and theoretical perspective. The two-dimensional finite difference computer code HEAT is used to predict temperature-time profiles at specified positions within an inert filled SCB. These predictions are then compared with temperatures obtained from thermocouple measurements made on the test apparatus. The general agreement is good and justifies the continued application of HEAT to the SCB. Some suggestions for further modifications to HEAT are made which would increase the accuracy of the calculation.

MATERIALS RESEARCH LABORATORY

Published by

Materials Research Laboratory
Cordite Avenue, Maribyrnong
Victoria, 3032 Australia

Telephone: (03) 319 3887
Fax: (03) 318 4536

AR No. 006-361

APPROVED FOR PUBLIC RELEASE

Authors

D.A. Jones

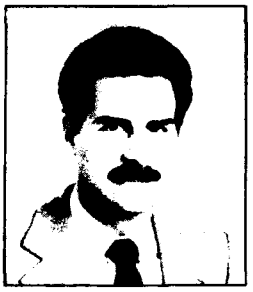

David Jones graduated from Monash University in 1972 with a BSc (Hons). He obtained his PhD from Monash in 1976. His thesis was titled "Anisotropic diffusion in the Townsend-Huxley experiment". After working at Strathclyde University, London University and the University of New South Wales he joined MRL in 1983. He has worked on the numerical modelling of shaped charge warheads and slapper detonator devices. From February 1987 to May 1988 he was a Visiting Scientist at the Laboratory for Computational Physics and Fluid Dynamics at the Naval Research Laboratories in Washington DC. While there he worked on advanced computational fluid dynamics.

R.P. Parker

Robert Parker graduated Dip App Chem from Ballarat School of Mines and Industries in 1968, and joined MRL in that year. He has worked exclusively on explosive materials; his present major areas of interest are cookoff of explosives and PBX formulations.

Contents

Heat Flow Calculations for the Small-Scale Cookoff Bomb Test

1. Introduction

A Super Small-scale Cookoff Bomb (SSCB) test facility has recently been established at MRL to provide data on the cookoff behaviour of energetic materials [1]. This test is suitable for explosive samples having a mass of about 20 g. The behaviour of explosive samples of considerably larger mass (up to 700 g) is evaluated using the Small-scale Cookoff Bomb (SCB) test [2]. The development of an SCB test at MRL is well advanced.

As part of the program to assess the cookoff behaviour of both existing and new explosive formulations at MRL we have made some preliminary heat flow calculations for the MRL SCB test apparatus. The calculations were performed with the HEAT computer code [3] to ascertain the suitability of the code for modelling the thermal environment in the SCB test.

HEAT is a reactive multi-material finite difference Fortran computer code for the solution of the diffusion equation in two-dimensional axisymmetric cylindrical geometry. It allows a maximum of three separate nested materials, and in a typical application the innermost material will be an explosive. HEAT therefore allows the innermost material to undergo a change in phase, and also to decompose via zero order Arrhenius kinetics.

The design of the SCB is shown in Figure 1. It is constructed from a single steel cylinder with a welded steel base. The upper section of the cylinder is threaded to allow it to be sealed by a screw-on steel cap. The SCB is then placed between two 127 mm square, 12.7 mm thick steel plates which are secured by four bolts. A small air gap exists between the upper surface of the explosive and the steel cap. Numerical modelling of the temperature distribution within the SCB therefore requires a computer code with the capability of simulating heat flow through the steel cylinder, the explosive, and the air gap. HEAT can model three nested materials and can be adapted to the geometry shown in Figure 1, and was therefore used for our numerical modelling of heat transfer in cookoff bomb tests by simulating the heat flow in the SCB. Numerical simulation of heat flow in the SSCB will be discussed in a future report.

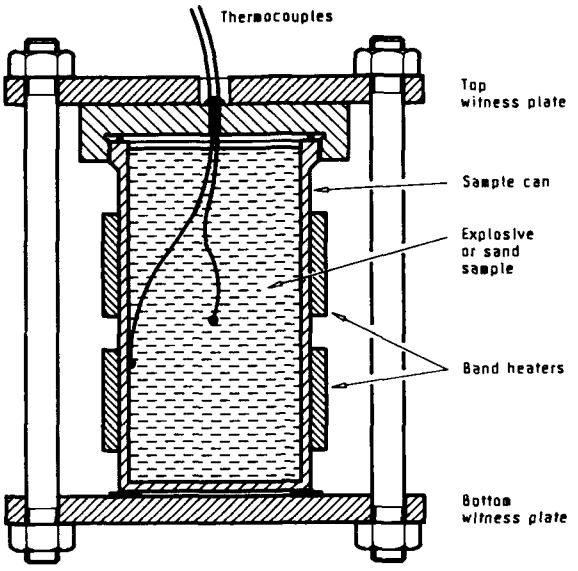

Figure 1: Small-scale Cookoff Bomb (SCB).

HEAT was originally developed to study the transient heating of a shell within a hot gun barrel. It employs the cylindrical geometry of a shell, with the boundary conditions imposing a time-independent temperature profile over the top and bottom surfaces of the outermost material. A time dependent programmed temperature is allowed along the curved cylindrical surface. Preliminary experimentation with the SCB using an inert explosive replacement and typical heating rates showed that the SCB behaviour was not compatible with the assumption of a time independent temperature profile over the end surfaces. Heat loss over these surfaces from both radiation and convection was also noted. Changes to the code were therefore made to alter the boundary conditions over these surfaces to allow a time dependent variable temperature profile and heat losses due to both radiation and convection. Because of the method used to solve the finite difference equations and the nonlinear nature of the radiation boundary condition, this entailed making quite detailed changes to the code. These changes are described in Section 2, along with the procedure we used to estimate realistic values for both the emissivity and heat transfer coefficient for the steel surfaces of the SCB.

To provide an experimental data base for comparison with the code calculations a series of SCB test runs was made using sand as an inert explosive substitute. Two Type K thermocouples were used in each test to record the temperature at various locations within the SCB; typically these were at the

sand/steel interface, and either the centre of the sand, or the surface of the steel cap. These locations are indicated on the schematic of the SCB in Figure 1. The thermocouples were connected to dedicated thermocouple amplifiers and the output from these amplifiers was then recorded using a strip chart recorder.

In order to obtain accurate estimates of the surface heat transfer coefficient and emissivity of the SCB surface a further series of test runs was made on a solid steel cylinder having approximately the same dimensions as the SCB. Up to nine thermocouples were used in each of the runs to measure temperature at various positions and depths into the cylinder, and the temperatures were recorded using a DT 100 Datataker.

In Section 4 a comparison is made between the HEAT code simulations and selected experimental records from the above two series of runs. In general the agreement is good, and justifies the continued application of HEAT to the numerical simulation of the SCB. The agreement is not perfect, however, and in most cases there are differences of the order of 10°C in some sections of the temperature-time records. A possible reason for this discrepancy is the neglect of the temperature dependence of the thermal diffusivity of each of the materials. This is also discussed further in Section 4. In Section 5 we summarize our results, and discuss directions for future work.

2. *HEAT Code Modifications*

The HEAT code has previously been described in detail [3]. It is a finite difference code which solves the partial differential equation describing time dependent thermal conduction with an internal heat source, i.e.

$$\frac{\partial T}{\partial t} = \frac{\lambda}{\rho C_p} \nabla^2 T + S \qquad (1)$$

where T is the temperature, ρ the density, λ the thermal conductivity, and C_p the specific heat at constant pressure. S is the source term representing internal heat generation due to thermal decomposition of the explosive. In the calculations described here we consider only inert materials and so have set S equal to zero. The combination $\lambda/(\rho C_p)$ is called the thermal diffusivity of the material. The value of this parameter determines the time dependence of the temperature distribution within the material.

Equation (1) is solved in two-dimensional axisymmetric cylindrical geometry with r and z representing displacements in the radial and axial directions respectively. A second order Forward-Time Centred-Space (FTCS) scheme is used to discretize the equations [4], and then the resulting set of algebraic equations is solved using the Alternating Direction Implicit (ADI) method [5]. This is a combination of implicit and explicit methods which solves the equations in two passes during one time step. In the first pass the partial derivatives in one direction (say z) are replaced by a finite difference expression in terms of known values of T (explicit), while the remaining partial derivatives

(r direction) are replaced by finite difference expressions in terms of unknown values (implicit). In the second pass the z direction is made implicit and the r direction explicit. The ADI method has several advantages over alternative finite-difference schemes: (a) the resulting sets of equations have a simple tridiagonal matrix form and so can easily be solved and (b) the equations are reported [4-6] to have stable solutions for any combination of time step size and spatial cell size.

In our early experimentation with HEAT we found that it was possible to choose combinations of Δt, Δr and Δz which gave unstable solutions for the temperature profiles and led to negative values for the absolute temperature. In all cases we were able to trace the origin of these unstable solutions to the presence of boundaries between different materials. While the ADI method is known to be unconditionally stable within a given material it is perhaps not surprising that this stability breaks down at an interface because the finite difference schemes used in HEAT are second order within the material, but only first order at the interface. The original report [3] noted this problem and gave guidelines for the avoidance of the unstable solutions. In particular, it was recommended that at least 10 computational cells span a given material in any one direction. This has forced us to use a very fine finite difference grid to model the SCB, but by complying with this guideline, and using realistic values for Δt, we have avoided the occurrence of unstable solutions.

The boundary conditions in the original version of HEAT consisted of a fixed temperature along the top and bottom of the finite difference grid and a prescribed time-dependent temperature over the outer curved surface. While this was adequate for the original problems to which HEAT was applied it was considered unsuitable for modelling either the SCB or SSCB as it made no allowance for thermal losses due to radiation, conduction or convection from the top and bottom surfaces of the apparatus. Consequently we have modified HEAT so that the temperatures along the top and bottom of the finite difference grid are determined by a boundary condition of the form

$$\frac{\partial T}{\partial n} = -\frac{h}{\lambda}[T_B - T_A] - \frac{\varepsilon\sigma}{\lambda}[T_B^4 - T_A^4] \qquad (2)$$

where n is the outward normal to the surface. The surface heat transfer coefficient is h, ε is the emissivity of the material, σ is the Stefan-Boltzmann constant, and T_B and T_A represent the temperature on the boundary and the ambient temperature of the surrounding medium (air) respectively. The first term on the right of equation (2) represents convective heat loss, while the second term represents heat loss due to thermal radiation.

To implement equation (2) we used the concept of a fictitious node point F outside the surface of the SCB. When the finite difference approximation to equation (1) is applied to a boundary node B this automatically introduces the temperature T_F at the fictitious point. By applying a central difference approximation to $\partial T/\partial n$ at the boundary node B, a second equation is obtained which also contains the temperature at the fictitious node point. T_F is then eliminated between these two equations and a single equation for the unknown

T_B is then obtained.

The solution of the equation for T_B is complicated by the nonlinearity of the second term on the right of equation (2). We resolved this problem by linearizing the term using the following approximation,

$$T_B^4 \approx T_{B,O}^4 + 4\,T_{B,O}^3\,(T_B - T_{B,O})$$

$$= 4\,T_{B,O}^3\,T_B - 3\,T_{B,O}^4 \qquad (3)$$

where $T_{B,O}$ is the temperature at the boundary node at the previous time step. This procedure is used and recommended by Croft and Lilley [6].

Although the replacement of the fixed temperature boundary condition by a condition on the gradient of the temperature at the boundary as given by equation (2) would appear to be fairly straightforward, it is worth emphasizing that this resulted in substantial changes to parts of the HEAT code. In particular, all Fortran DO LOOPS along the axial direction were altered to allow for additional points along the top and bottom of the grid. In addition, the arrays involved in the tridiagonal matrix calculations had to be expanded to allow for these additional points.

Before using the new version of HEAT, realistic values for the coefficients h and ε had to be determined. We did this by taking a solid steel cylinder of axial length 125 mm and diameter 70 mm, attaching the SCB heating bands to it, and rapidly heating it to a temperature of 236°C. We then monitored the temperature of the block using several thermocouples at various depths into the block and recorded the temperature-time history until the block had almost reached ambient temperature again. Because of the high thermal conductivity of the steel and the comparatively long time scale of the cooling curve all points within the block have the same temperature *at any given time* (the thermocouple measurements confirmed this). This temperature is given by the solution of the following ordinary differential equation.

$$mC_p\,(dT/dt) = -hA(T - T_A) - \varepsilon\sigma A(T^4 - T_A^4) \qquad (4)$$

where A is the total surface area of the cylindrical block.

Using the values $\rho = 7680$ kg/m^3, $Cp = 485$ J/kg.K, and $T_A = 20$°C we solved equation (4) using a simple fourth order Runge-Kutta integration routine for various realistic estimates of the coefficients h and ε. Figure 2 shows the solution obtained using $h = 7$ W/m^2 K and $\varepsilon = 0.8$ and also the experimental points. The agreement is excellent, and we have used these values for h and ε in all the calculations described in this report. The value for h obtained here is also in excellent agreement with the value quoted in [8] for heat transfer from the surface of a cylindrical steel barrel over a similar temperature range. It should be noted that, since the value of ε depends significantly on the oxidation state of the metal surface, the value of ε obtained for the solid steel block will not necessarily be valid for the surface of the steel cap used on the SCB, or the surfaces of the confining steel end plates. This is not crucial

however as we noted very little change to the curve shown in Figure 2 when we varied ε over the range 0.7 to 0.9. This simply reflects the fact that convection, rather than radiation, is the more important heat loss mechanism in the temperature range shown in Figure 2. The calculations described in the next section will also show that heat loss through the ends of the SCB has only a minor effect on the temperature distribution within the SCB, and so very accurate determinations of ε and h are not required.

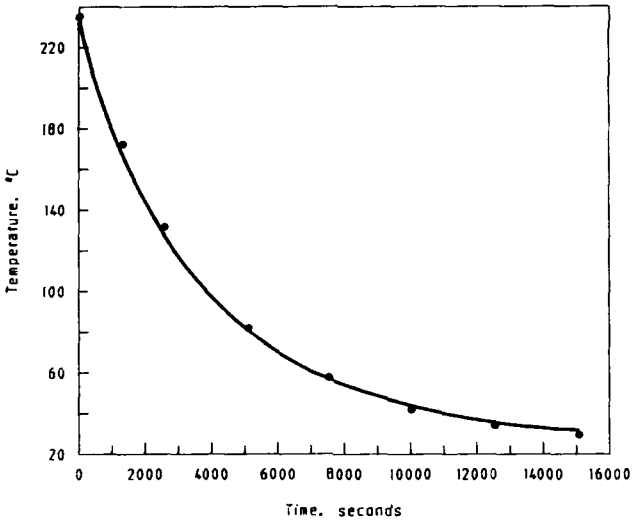

Figure 2: Cooling curve for solid steel cylinder. Solid line – from solution of ordinary differential equation describing heat loss due to convection and radiation. Filled circles – experimental points.

3. *Experimental Measurements*

Before discussing any of the HEAT code simulations we first describe some of the experimental results for the SCB using sand as an explosive substitute. The upper curve in Figure 3a shows the temperature of the sand/steel interface at a point located at about half the height of the cylinder, while the lower curve is the temperature on the top surface of the SCB approximately at the centre. The Variac potential was set to 120 volts and the upper curve shows that power was supplied for about 550 seconds and then switched off. This heated the sand/steel interface to approximately 350°C, and then very rapid cooling of the steel cylinder occurred. The temperature on the upper surface of the SCB rose very slowly however, reaching a temperature of only 80°C when the sand/steel

interface was at 350°C. It then continued to rise very slowly for some time after the power supply was removed. The very low temperature on the upper surface of the SCB was unexpected and so we ran several more tests to try to identify the cause of this behaviour. Figure 3b is a repeat run with the SCB empty, and similar results were obtained. We then removed the screw-on cap and turned the SCB upside down. Figure 3c again shows the temperature on the inside of the steel cylinder (the upper curve), while the initially lower curve is the temperature recorded at the centre of the top surface of the upturned SCB (i.e. what is normally the base). The two temperatures are now much closer and the temperature difference between the two points is due to the finite time taken for the heat to diffuse from the heating bands to the upper surface (we describe this in more detail when discussing Figure 7). These results are important because they show that the large mass of steel in the cap has a significant effect on the heat flow and temperature distribution within the SCB, and indicate that the effect of the massive steel witness plates should also be included in any numerical simulation of the full SCB assembly.

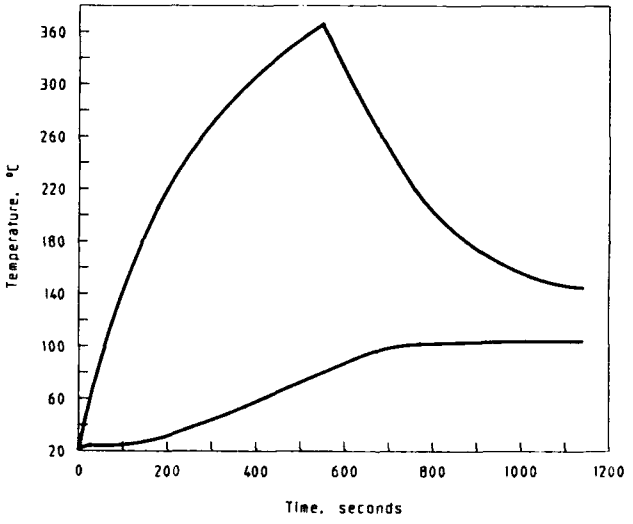

Figure 3a: Temperature measured at two locations within an SCB filled with sand. Upper curve – temperature at the sand/steel interface at a position halfway up the height of the cylinder. Lower curve – temperature on the top surface of the SCB cap at the approximate centre point.

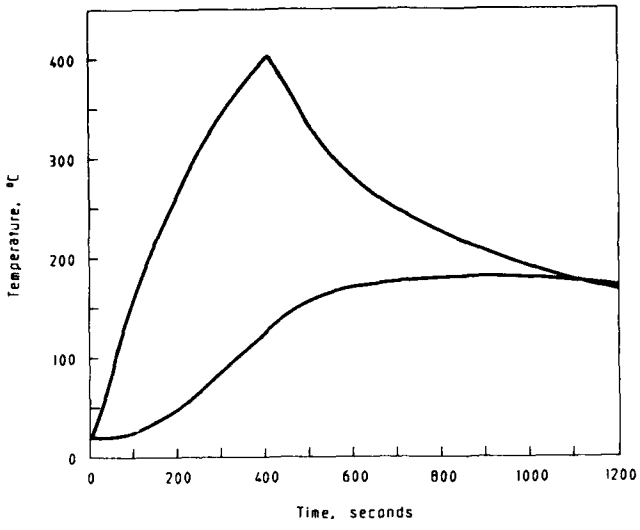

Figure 3b: As for Figure 3a, except that the sand has been removed and the SCB is simply air-filled.

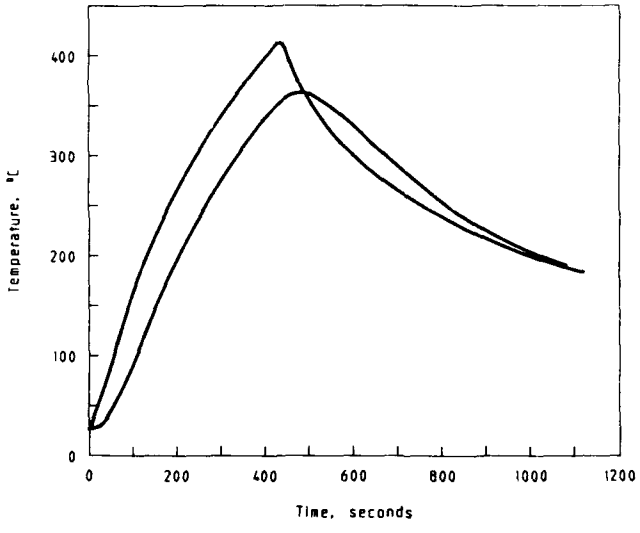

Figure 3c: Temperatures measured at two locations on an empty, inverted SCB with the screw cap removed. The (initially) upper curve denotes the temperature on the inside surface of the steel cylinder, while the (initially) lower curve is the temperature recorded at the centre of the top surface of the upturned SCB.

We have also found similar behaviour for the solid steel cylindrical block described in the previous section. The SCB heating bands were placed around the cylinder (in exactly the same position as when applied to the SCB, refer to Figure 1) and connected to a 240 volt power supply for 120 seconds. The solid upper and lower curves in Figure 4 are the temperatures recorded on the curved surface of the block midway between the two heating bands and the temperature at the centre of the top surface of the block, respectively. The dashed upper and lower curves are the temperatures recorded at the same locations under identical experimental conditions for another run. The difference between the solid and dashed curves illustrates the degree of reproducibility between the two runs. The SCB heating bands do not cover the entire curved surface of the cylinder; there is an 8 mm gap between the top edge of the band and the top surface of the block. The broken upper and lower curves in Figure 4 are the temperatures recorded again at the same locations, only this time the top surface of the upper heating band has been moved up to be flush with the top surface of the block. In this case the side temperature is lower and the surface temperature higher (after a certain time) because of the relative placement of the heating band. These results indicate that very accurate numerical simulations of the temperature distribution within the SCB will require further modification to the HEAT code to allow the finite size of the heating bands to be specified.

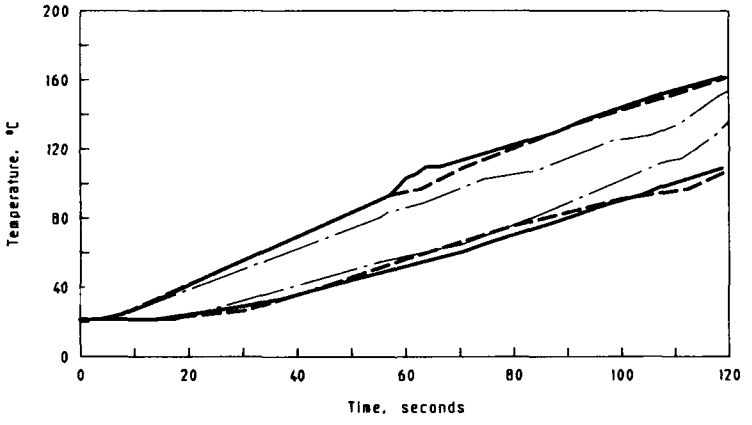

Figure 4: Temperatures measured at several locations on a solid steel cylinder as a function of time. The cylinder has the same dimensions as the SCB and is heated using the SCB heating bands. The solid upper and lower curves are the temperatures recorded on the curved surface of the block midway between the two heating bands, and the temperature at the centre of the top surface of the block, respectively. The dashed upper and lower curves are the temperatures recorded at the same locations for a replicate run. The broken upper and lower curves are the temperatures recorded again at the same locations, only this time the top surface of the upper heating band has been moved up to be flush with the top surface of the block.

4. *HEAT Code Calculations*

Before using HEAT to model the complexity of the multi-material SCB we first applied the code to the simpler problem of modelling the temperature distribution within the solid cylindrical steel block. HEAT requires as input a prescribed time-dependent temperature profile along the outer curved surface. For the solid steel block we used an average of the two uppermost curves shown in Figure 4. These data are denoted by the upper solid curve in Figure 5. The filled circles denote experimental values for the temperature on the surface and are averages of the two lowermost curves in Figure 4, while the lower solid curve is the HEAT code result. The computational grid consisted of 125 cells in the axial direction and 35 cells in the radial direction, with $\Delta z = \Delta r = 1$ mm, and $\Delta t = 10$ s. The density and specific heat were held constant at 7860 kg/m^3 and 490 J/kg.K respectively, and the thermal conductivity was varied to give the best possible fit to the experimental points. This resulted in a value for λ of 40.0 W/m.K. Thermal conductivity varies greatly between steels of different types, and the value determined here is consistent with values quoted in the literature [7, 8].

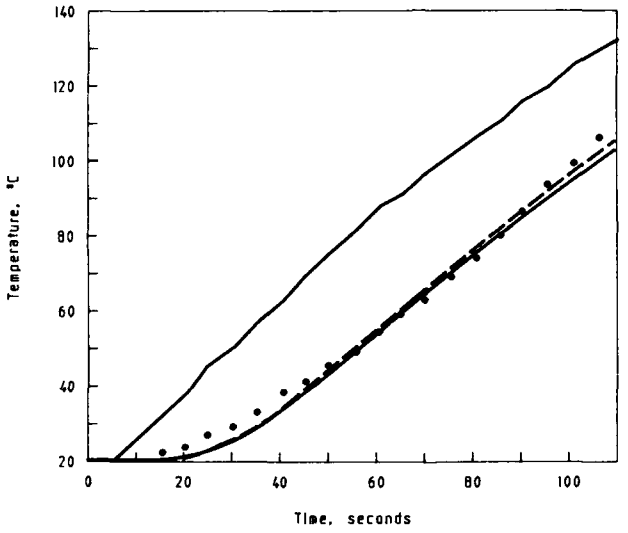

Figure 5: Comparison of calculated and measured temperatures for the solid cylindrical block. The upper solid curve is the average measured temperature on the side of the block and is used as the input surface temperature for the HEAT code simulation. The filled circles denote temperatures measured at the centre of the top surface of the block, and the lower solid curve is the HEAT code simulation. The dashed line represents temperatures at the centre of the top surface calculated from a one-dimensional code.

Although there appears to be reasonable agreement between the predicted and experimental temperature-time curves shown in Figure 5, closer examination shows that the two curves have quite different shapes, indicating that some of the assumptions used in the numerical model may not be valid. One such assumption is that the thermal properties of the materials are temperature independent. This is discussed further in the next section. The approximate agreement between the two curves does allow us to conclude however that the temperature difference between the top and side surfaces of the SCB observed in Figure 5 is simply due to the finite time needed for the heat to diffuse from the heating bands to the upper surface of the block.

Experimentation with the code showed that the results were insensitive to the values used for ε and h, implying that heat losses through the ends of the cylinder were not responsible for determining the temperature distribution over the top and bottom surfaces. This was checked by calculating the surface temperature using a simple one-dimensional explicit code, and the result is shown by the dashed line in Figure 5. The temperatures calculated using the one-dimensional code are slightly higher than those calculated using HEAT, but the difference is at most a few degrees C°. This clearly shows that the heat flow along the axis of the cylinder has little effect on the calculated temperatures, and demonstrates that the primary influence on the surface temperature profile is the energy input from the heating bands on the surface of the cylinder, and their location from the point at which the temperature is measured. The appropriate HEAT code boundary conditions over the top and bottom surfaces for this simulation are evidently

$$\partial T/\partial n = 0, \qquad (5)$$

rather than equation (2), although the changes to the coding to implement equation (5) are as involved as those required to implement equation (2). It should also be noted that this particular simulation was conducted at a very rapid heating rate, and while the radiative and convective heat loss terms are insignificant for this particular heating regime, this will not necessarily be the case for the very much slower heating rates used for slow cookoff studies, where the explosive events can take on the order of 20 hours to occur.

We now consider the temperature within an inert filled SCB. Figure 6 shows the temperature measured at the sand/steel interface (the initially upper solid line), the temperature measured at the centre of the sand fill (the filled circles), and the HEAT code calculation for the temperature at the centre of the sand using two different values for the thermal conductivity of the sand (lower solid line, λ = 0.25 W/m.K; dashed line λ = 0.27 W/m.K). The values of the physical constants used for the three materials (sand, steel and air) are listed in Table 1. The discontinuity in the slope of the curve for the temperature measured in the centre of the sand is caused by the vapourization of adsorbed water from the sand at 100°C. This phase change effect is not modelled by HEAT and the computed curve cannot reproduce this discontinuity. Provided comparisons between computed and experimental curves are made above this temperature however this will not affect the results to be discussed here.

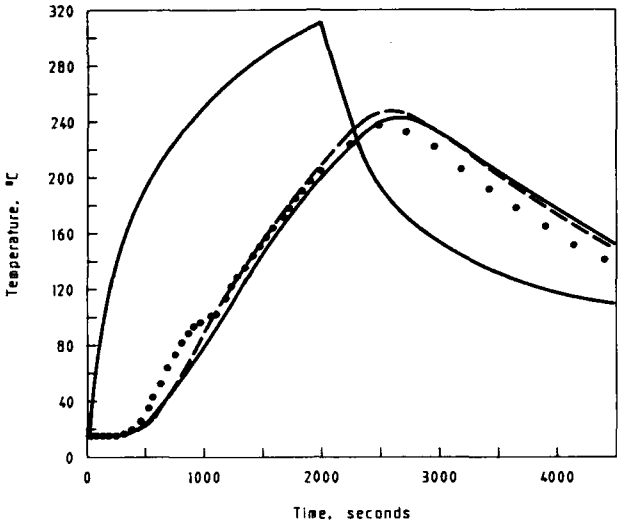

Figure 6: Comparison of calculated and measured temperatures for the inert filled SCB. The (initially) solid upper curve is the temperature measured at the sand/steel interface which is used as the input temperature for HEAT. The filled circles denote the measured temperature at the centre of the sand, and the (initially) lower solid curve and the dashed curve represent the HEAT code results calculated using λ (sand) equal to 0.25 and 0.27 W/m.K respectively.

The agreement between calculated and experimental temperatures in Figure 6 is reasonable, and if the errors in the experimental points are considered to have the same magnitude as those shown in Figure 4 then the agreement is very close, but not quite exact. The two curves calculated using slightly different values of thermal conductivity show that it is possible to improve agreement in some parts of the temperature-time domain, but this then leads to worse agreement in other parts. It was found impossible to vary any of the material parameters in such a way as to improve the overall agreement. We attribute the inability of HEAT to predict the temperature across the entire time period to the neglect of the temperature variation of the thermal parameters. We subsequently measured the specific heat of the sand in this particular test using the differential scanning calorimetry method and found it to vary by 20% over the temperature range 100°C to 200°C (see Table 2). We anticipate that if HEAT were modified to include the temperature dependence of the thermal conductivity and heat capacity then the agreement shown in Figure 6 would be considerably improved.

Table 1: Material Parameters for Inert Filled SCB

Sand:	λ	=	0.25 W/m.K
	C_p	=	1108 J/kg.K
	ρ	=	1410 kg/m^3
Air:	λ	=	0.03 W/m.K
	C_p	=	1004 J/kg.K
	ρ	=	1.2 kg/m^3
Steel:	λ	=	40.0 W/m.K
	C_p	=	490 J/kg.K
	ρ	=	7860 kg/m^3

Table 2: Specific Heat of Inert (Sand)

Temperature (K)	C_p (J/kg.K)
370	825
380	843
420	896
430	917
460	944
470	972

We have also calculated the temperature at the centre of the sand using the one-dimensional explicit code and found exact agreement with the two-dimensional HEAT results. This illustrates that the heat loss through the end surfaces of the cylinder has little effect on the temperature at this location and for this heating rate, and that the primary influence on the temperature is provided by the energy flowing into the sand from the heating bands.

One final illustration of the above two points is provided by Figure 7. This shows a comparison between the calculated and predicted temperatures for the SCB for the situation described in relation to Figure 3c, i.e. the SCB is empty and inverted. The initially upper solid curve is the temperature on the inside wall, the filled circles the temperature measured on the top of the base at the centre, and the initially lower solid curve the HEAT code prediction. Again the overall agreement between calculated and measured temperatures is only fair; there is exact agreement for early times, and again for late times (although this may be fortuitous), but it was found impossible to vary the thermal parameters within realistic limits and produce agreement everywhere.

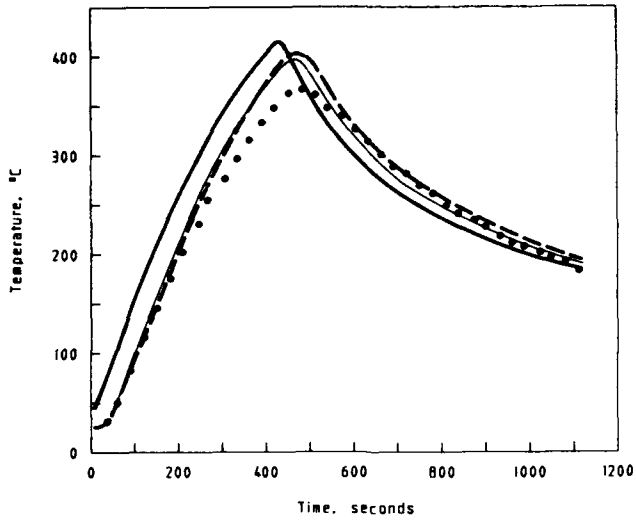

Figure 7: Comparison of calculated and measured temperatures for the SCB for the configuration described in Figure 3c. The (initially) upper solid curve is the temperature on the inside wall of the SCB, the filled circles are the measured temperatures on the top of the SCB, and the (initially) lower solid curve is the HEAT code simulation of this temperature. The dashed curve is the temperature at the same point calculated using a one-dimensional code.

The slightly larger discrepancy between the calculated and experimental points in the midpoint of the range may also be due to the effect of convective heat flow in the air contained within the SCB. This undoubtedly occurs in the early stages of heating but has not been included in the simulation, which may have led to an overall shift in the position of the computed curve and exaggerated the discrepancy at the midpoint. The temperature has also been calculated using the one-dimensional code and this is shown by the dashed line. Again, the results are very similar.

5. Discussion and Conclusion

The experimental results and numerical simulations described in the previous section allow us to make the following observations:

(a) Accurate numerical simulation of the temperature distribution within some parts of the SCB will not be possible with the existing version of HEAT. We are referring in particular here to the temperature distribution on the surface of the screw-on cap shown in Figures 3a and 3b. A more accurate prediction could be made by modifying parts of HEAT to allow the driving temperature to be applied only to those parts of the finite difference grid which are in contact with the heating bands, and then allowing the remainder of the curved surface to lose heat through radiation and convection. This would require extensive changes however, and may not be necessary for our purposes.

(b) The temperature within the explosive sample in an SCB may well be determined to within an acceptable accuracy by neglecting heat flow along the axis of the SCB and using a one-dimensional code to calculate temperature along the radial direction. This could be investigated further using HEAT to calculate axial temperature profiles, and also with additional thermocouple measurements at selected points within the explosive substitute.

(c) Accurate prediction of the temperature-time profiles within the explosive will require a computer code which allows for the detailed temperature dependence of the explosive's thermal properties.

Bearing the above observations in mind, we make the following recommendations:

(i) Several more runs should be made on the inert filled SCB using additional thermocouples to obtain a better knowledge of the temperature distribution within the explosive.

(ii) Additional HEAT code simulations should be performed to investigate the temperature variation in the axial direction.

(iii) The temperature dependence of the thermal parameters for the inert fill should be determined accurately.

(iv) A one-dimensional heat flow code which takes into account the temperature dependence of the material properties should be written and then applied with the parameters determined in (iii) above to see if improved agreement between calculated and experimental temperatures can be obtained.

(v) The origin of the instabilities which occur for some combinations of Δr, Δz and Δt should be investigated more thoroughly. This could most easily be performed by considering the stability of the finite difference scheme across an interface using a one-dimensional version of the code.

6. Acknowledgements

We thank Dr Dan Whelan for determining the temperature dependence of the specific heat of the sand and for advice on thermal properties in general. We thank Mr John Rusjan (a vacation scholar during the period December 1988 to February 1989) for assistance with the numerical simulations during the early stages of this work, and we particularly thank Mr John Waschl, the originator of the HEAT code, for carefully checking many of our calculations and our changes to the HEAT coding.

7. References

1. Parker, R.P. (1989).
Establishment of a super small-scale cookoff bomb (SSCB) test facility at MRL (MRL Technical Report MRL-TR-89-9). Maribyrnong, Vic.: Materials Research Laboratory.

2. Pakulak, J.M. Jr. (1984).
USA small-scale cookoff bomb (SCB) test. *Minutes of 21st Department of Defense Explosives Safety Board Explosives Safety Seminar*, Houston, TX.

3. Waschl, J.A. (1987).
A reactive multi-material first order numerical model for heat conduction in cylindrical coordinates (MRL Report MRL-R-1065). Maribyrnong, Vic.: Materials Research Laboratory.

4. Fletcher, C.A.J. (1988).
Computational techniques for fluid dynamics, Volume 1. *Springer Series in Computational Physics*, Springer-Verlag.

5. Smith, G.D. (1978).
Numerical solution of partial differential equations: finite difference methods. *Oxford Applied Mathematics and Computing Science Series*, 2nd edition. Oxford University Press.

6. Croft, D.R. and Lilley, D.G. (1977).
Heat transfer calculations using finite difference equations. London: Applied Science Publishers Ltd.

7. *CRC Handbook of chemistry and physics.* (Ed.) R.C. Weast, 64th edition, 1984/84. Florida: CRC Press Inc.

8. *Textbook of ballistics and gunnery*, Volume 1 (1987).
London: Her Majesty's Stationery Office.

SECURITY CLASSIFICATION OF THIS PAGE **UNCLASSIFIED**

DOCUMENT CONTROL DATA SHEET

REPORT NO.	AR NO.	REPORT SECURITY CLASSIFICATION
MRL-TR-91-12	AR-006-361	Unclassified

TITLE

Heat flow calculations for the small-scale cookoff bomb test

AUTHOR(S)
D.A. Jones and R.P. Parker

CORPORATE AUTHOR
Materials Research Laboratory
PO Box 50
Ascot Vale Victoria 3032

REPORT DATE	TASK NO.	SPONSOR
May, 1991	DST 88/090	DSTO

FILE NO.	REFERENCES	PAGES
G6/4/8-4006	8	23

CLASSIFICATION/LIMITATION REVIEW DATE

CLASSIFICATION/RELEASE AUTHORITY
Chief, Explosives Division

SECONDARY DISTRIBUTION

Approved for public release

ANNOUNCEMENT

Announcement of this report is unlimited

KEYWORDS

SCB
Heat
Numerical simulation
Heat conduction
Heat transfer
Boundary layers
Boundary interfaces

ABSTRACT

This report describes the temperature distribution within the Small-scale Cookoff Bomb (SCB) test apparatus from both an experimental and theoretical perspective. The two-dimensional finite difference computer code HEAT is used to predict temperature-time profiles at specified positions within an inert filled SCB. These predictions are then compared with temperatures obtained from thermocouple measurements made on the test apparatus. The general agreement is good and justifies the continued application of HEAT to the SCB. Some suggestions for further modifications to HEAT are made which would increase the accuracy of the calculation.